Article

Human Tryptophan Dioxygenase: A Comparison to Indoleamine 2,3-Dioxygenase

Dipanwita Batabyal, and Syun-Ru Yeh

J. Am. Chem. Soc., **2007**, 129 (50), 15690-15701 • DOI: 10.1021/ja076186k

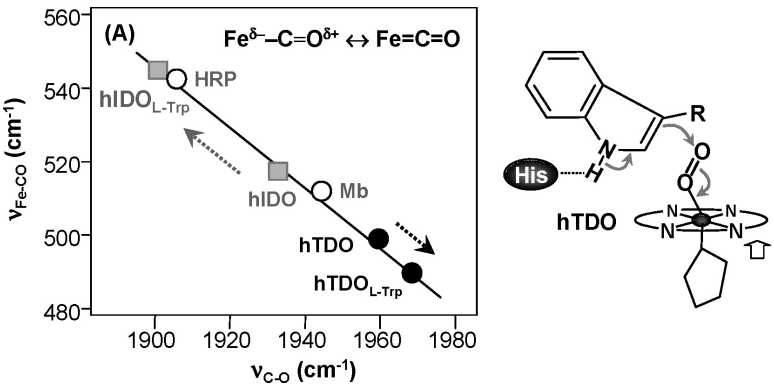

More About This Article

Additional resources and features associated with this article are available within the HTML version:

- Supporting Information
- Links to the 8 articles that cite this article, as of the time of this article download
- Access to high resolution figures
- Links to articles and content related to this article
- Copyright permission to reproduce figures and/or text from this article

View the Full Text HTML

J|A|C|S
ARTICLES
Published on Web 11/21/2007

Human Tryptophan Dioxygenase: A Comparison to Indoleamine 2,3-Dioxygenase

Dipanwita Batabyal and Syun-Ru Yeh*

Contribution from the Department of Physiology and Biophysics, Albert Einstein College of Medicine, 1300 Morris Park Avenue, Bronx, New York 10461

Received August 20, 2007; E-mail: syeh@aecom.yu.edu

Abstract: In contrast to the diverse superfamily of monooxygenases, there are only two classes of heme-containing dioxygenases in humans. One is tryptophan 2,3 dioxygenase (hTDO), and the other is indoleamine 2,3-dioxygenase (hIDO), both of which catalyze the oxidative degradation of Trp to *N*-formyl kynurenine. Although hTDO and hIDO catalyze the same reaction, they engage in distinct physiological functions. The molecular properties of hTDO, unlike hIDO, have never been explored in the past. Here, we report the first structural and functional characterization of hTDO with resonance Raman and optical absorption spectroscopies. We show that the proximal Fe-His stretching frequency of hTDO is 229 cm^{-1}, 7 cm^{-1} lower than that of hIDO, indicating its weaker imidazolate character as compared to hIDO. In the CO derivative of the L-Trp-bound enzyme, the Fe−CO stretching and C−O stretching frequencies are 488 and 1972 cm^{-1}, respectively, suggesting that L-Trp binds to the distal pocket with its C_2-C_3 double bond facing the heme-bound ligand, in contrast to hIDO, in which the indole NH group forms an H-bond with the heme-bound ligand. Moreover, the K_m values of hTDO for D-Trp and L-Trp are similar, but the k_{cat} value for D-Trp is 10-fold lower than that for L-Trp. In contrast, in hIDO, the K_m value for D-Trp is 700-fold higher than L-Trp, whereas the k_{cat} values are comparable for the two stereoisomers. Taken together, the data indicate that the initial deprotonation reaction of the indole NH group in hTDO is carried out by the evolutionarily conserved distal His, whereas that in hIDO is performed by the heme-bound dioxygen; in addition, the stereospecificity of hTDO is determined by the efficiency of the dioxygen chemistry, whereas that in hIDO is controlled by the substrate affinity.

Introduction

Human tryptophan 2,3-dioxygenase (hTDO) is a hepatic heme-containing enzyme that catalyzes the conversion of L-Tryptophan (L-Trp) to *N*-formylkynurenine (NFK), the initial and rate-determining step of the kynurenine pathway, by inserting both oxygen atoms of molecular oxygen across the C_2-C_3 double bond of the indole moiety of Trp as illustrated in the left panel of Scheme 1.[1−6] In liver, another enzyme, formamidase, deformylates NFK to kynurenine, which acts as a precursor for the synthesis of nicotinic acids, NAD and NADP.[7] The majority of our dietary Trp is metabolized by hTDO through the kynurenine pathway, and a small amount of it is used to synthesize the neurotransmitter serotonin.[8] Consequently, hTDO plays a critical role in determining the relative Trp flux in the serotonergic and kynurenine pathways.

In addition to humans, TDO has also been found in other mammals, such as rat and mouse, as well as in mosquitoes and bacteria.7,9-14 Although TDO from rats and bacteria have been extensively studied,[4,6,7,12−18] the crystal structure of TDO has only been recently resolved by Ealick *et al.*[19] and Tong *et al.*,[10] independently, based on the isoforms from *Ralstonia metallidurans* (rmTDO) and *Xanthomonas campestris* (xcTDO), respectively. The two bacterial TDOs show considerable sequence homology with hTDO.[10] In both structures, TDO was found in a tetrameric form with one heme in each of the four monomers. The heme is coordinated by a proximal His residue

(1) Hayaishi, O. *J. Biochem.* (*Tokyo*) **1976**, *79*, 13−21.
(2) Hayaishi, O.; Takikawa, O.; Yoshida, R. *Prog. Inorg. Chem* **1990**, *38*, 75.
(3) Feigelson, O.; Brady, F. O. In *Molecular Mechanism of Oxygen Activation*; New York, 1974; pp 87−133.
(4) Schutz, G.; Feigelson, P. *J. Biol. Chem.* **1972**, *247*, 5327−5332.
(5) Greengard, O.; Feigelson, P. *J. Biol. Chem.* **1961**, *236*, 158−161.
(6) Sono, M.; Roach, M. P.; Coulter, E. D.; Dawson, J. H. *Chem. Rev.* **1996**, *96*, 2841−2888.
(7) Tanaka, T.; Knox, W. E. *J. Biol. Chem.* **1959**, *234*, 1162−70.
(8) Takikawa, O. *Biochem. Biophys. Res. Commun.* **2005**, *338*, 12−19.
(9) Greengard, O.; Feigelson, P. *J. Biol. Chem.* **1962**, *237*, 1903−1907.
(10) Forouhar, F.; Anderson, J. L.; Mowat, C. G.; Vorobiev, S. M.; Hussain, A.; Abashidze, M.; Bruckmann, C.; Thackray, S. J.; Seetharaman, J.; Tucker, T.; Xiao, R.; Ma, L. C.; Zhao, L.; Acton, T. B.; Montelione, G. T.; Chapman, S. K.; Tong, L. *Proc. Natl. Acad. Sci. U.S.A.* **2007**, *104*, 473−478.
(11) Li, J. S.; Han, Q.; Fang, J.; Rizzi, M.; James, A. A.; Li, J. *Arch. Insect Biochem. Physiol.* **2006**, *64*, 74−87.
(12) Ishimura, Y.; Nozaki, M.; Hayaishi, O. *J. Biol. Chem.* **1970**, *245*, 3593−3602.
(13) Schutz, G.; Chow, E.; Feigelson, P. *J. Biol. Chem.* **1972**, *247*, 5333−5337.
(14) Poillon, W. N.; Maeno, H.; Koike, K.; Feigelson, P. *J. Biol. Chem.* **1969**, *244*, 3447−3456.
(15) Ishimura, Y.; Nozaki, M.; Hayaishi, O. *J. Biol. Chem.* **1967**, *242*, 2574−2576 .
(16) Feigelson, P.; Brady, F. O.; McCray, J. A. *J. Biol. Chem.* **1973**, *248*, 5267−5271.
(17) Henry, Y.; Ishimura, Y.; Peisach, J. *J. Biol. Chem.* **1976**, *251*, 1578−1581.
(18) Makino, R.; Iizuka, T.; Sakaguchi, K.; Ishimura, Y. In *Oxygenase and Oxygenase Metabolism*; Nozaki, M., Ed.; Academic Press, Inc.: New York, 1982, pp 467−477.
(19) Zhang Y.; Kang, S. A.; Mukherjee, T.; Bale, S.; Crane, B. R.; Begley, T. P.; SE., E. *Biochemistry* **2007**, *46*, 145−155.

10.1021/ja076186k CCC: $37.00

Scheme 1

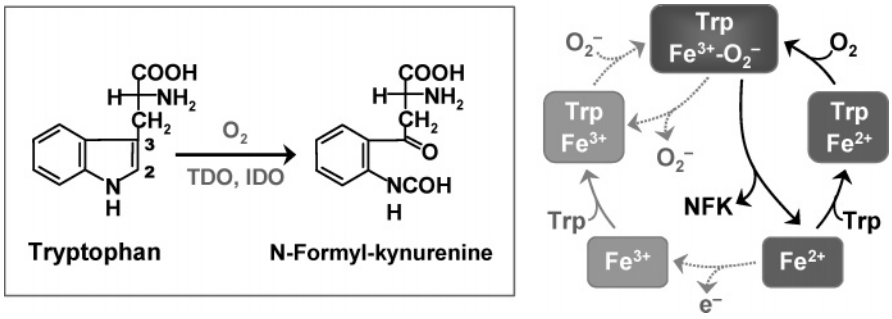

at the 240 position (numbering based on the xcTDO sequence hereafter), which is absolutely conserved in all TDOs. In the structure of the L-Trp-bound ferrous xcTDO, the carboxylate and ammonium groups of L-Trp form H-bonds with the protein matrix as well as a propionate group of the heme and a water molecule as shown in Figure 1. The indole ring, which lies perpendicular to the heme plane, is held in position by van der Waals contacts with several surrounding hydrophobic residues, including those from the same subunit and those from the N terminus of the adjacent subunit of the tetramer (see Figure S1 of the Supporting Information). Among these interactions, the amine group of the indole ring forms an H-bond with the side chain group of an evolutionarily conserved histidine at position 55 (Figure 1), which is important for the deprotonation reaction of L-Trp required for the dioxygenase activity as will be discussed in this article. Furthermore, the indole ring faces the sixth coordination site of the heme-iron, presumably poised for the dioxygen chemistry.

TDO was first discovered in rat liver extracts in 1936 by Kotake and Masayama.[20] It was later found that, in addition to TDO, there is a second enzyme that catalyzes the oxidative cleavage of the Trp.[21] This enzyme, named indoleamine-2,3-dioxygenase (IDO), was not identified and purified until three decades later.[22] Subsequent studies showed that, like TDO, IDO is also a heme-containing enzyme, despite the fact that it shares no sequence homology with TDO.[10,22] Additional work demonstrated that IDO exhibits several unique properties as compared to TDO: (1) IDO is a monomeric enzyme (MW ≈ 45 kDa), in contrast to the tetrameric structure of TDO (MW ≈ 167 kDa);[1,4,9,10,22,23] (2) IDO oxidizes L-Trp, D-Trp, and various indoleamine derivatives, in contrast to TDO, which is more specific to L-Trp;[1,6,23,24] (3) IDO is only present in mammals and is ubiquitously distributed in all tissues other than liver,[1,22,25] whereas TDO is present mostly in liver, and it is not only found in mammals, but also in mosquitoes and bacteria;[9−11] and (4) the expression of IDO is induced by IFN-γ and is closely linked to a wide spectrum of immune-related pathophysiological conditions,[6,8,25,26] in contrast to TDO, which is inducible by glucocorticoid hormones and is regulated by the availability of the physiological substrate, L-Trp.[27,28]

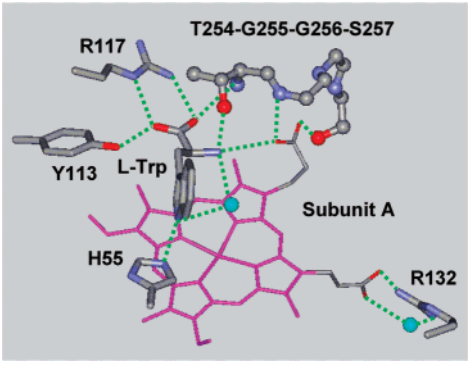

Figure 1. H-bonding interactions stabilizing the L-Trp in xcTDO. The PDB code is 2NW8. The green dotted lines represent H-bonds. The cyan spheres are water molecules.

The crystal structure of human IDO (hIDO) was reported last year by Shiro and co-workers.[29] The overall structure of hIDO shows two alpha-helical domains sandwiching the prosthetic heme group. Intriguingly, although there is no sequence homology between IDO and TDO, the large domain of IDO exhibits high structural similarity with TDO,[19] suggesting that the two dioxygenases may carry out the dioxygen chemistry by similar mechanisms. However, considerable evidence suggests the opposite: (1) IDO binds oxygen regardless of Trp, whereas TDO only binds oxygen in the Trp-bound derivative;[12,30] (2) the oxygen complex of IDO is readily oxidizable, whereas that of TDO is much less susceptible to autooxidation;[6,12,30] (3) the ferric derivative of IDO can react with superoxide to form the active oxy-complex, whereas that of TDO does not bind superoxide;[6,31] and (4) the binding of L-Trp in IDO retards CO binding, whereas it accelerates it in TDO.[16,30] In the reaction cycle shown in the right panel of Scheme 1, we highlight the major differences in the multiple turnovers catalyzed by TDO and IDO, in which the reaction path labeled by the dotted gray arrows takes place only in IDO, not TDO.

The recombinant hIDO enzyme can be easily expressed in *E. coli* and purified with high yield; as a result, the biochemical and biophysical properties of hIDO have been extensively investigated.[6,23,25,29,32−34] In contrast, hTDO has never been

(20) Kotake, Y.; Masayama, T. Z. *Physiol. Chem.* **1936**, *243*, 237.
(21) Kotake, Y.; Ito, N. *J. Biochem. (Tokyo)* **1937**, *25*, 71.
(22) Yamamoto, S.; Hayaishi, O. *J. Biol. Chem.* **1967**, *242*, 5260−5266.
(23) Shimizu, T.; Nomiyama, S.; Hirata, F.; Hayaishi, O. *J. Biol. Chem.* **1978**, *253*, 4700−4706.
(24) Hirata, F.; Hayaishi, O. *Biochem. Biophys. Res. Commun.* **1972**, *47*, 1112−1119.
(25) Muller, A. J.; Prendergast, G. C. *Curr. Cancer Drug Targets* **2007**, *7*, 31−40.
(26) Munn, D. H.; Mellor, A. L. *J. Clin. Invest.* **2007**, *117*, 1147−1154.
(27) Schutz, G.; Killewich, L.; Chen, G.; Feigelson, P. *Proc. Natl. Acad. Sci. U.S.A.* **1975**, *72*, 1017−1020.
(28) Schimke, R. T.; Sweeney, E. W.; Berlin, C. M. *J. Biol. Chem.* **1965**, *240*, 322−331.
(29) Sugimoto, H.; Oda, S.; Otsuki, T.; Hino, T.; Yoshida, T.; Shiro, Y. *Proc. Natl. Acad. Sci. U.S.A.* **2006**, *103*, 2611−2616.
(30) Taniguchi, T.; Sono, M.; Hirata, F.; Hayaishi, O.; Tamura, M.; Hayashi, K.; Iizuka, T.; Ishimura, Y. *J. Biol. Chem.* **1979**, *254*, 3288−3294.
(31) Hirata, F.; Ohnishi, T.; Hayaishi, O. *J. Biol. Chem.* **1977**, *252*, 4637−4642.
(32) Terentis, A. C.; Thomas, S. R.; Takikawa, O.; Littlejohn, T. K.; Truscott, R. J.; Armstrong, R. S.; Yeh, S. R.; Stocker, R. *J. Biol. Chem.* **2002**, *277*, 15788−15794.
(33) Papadopoulou, N. D.; Mewies, M.; McLean, K. J.; Seward, H. E.; Svistunenko, D. A.; Munro, A. W.; Raven, E. L. *Biochemistry* **2005**, *44*, 14318−14328.

explored *in vitro*, due to the technical difficulties associated with its tendency to aggregate in free solution and to form inclusion bodies when expressed in *E. coli*. By including L-Trp throughout the preparation steps, we were able to produce sufficient amounts of active recombinant hTDO enzyme for spectroscopic studies (Batabyal et al., manuscript in preparation). Here, we report the first thorough structural and functional characterization of hTDO with resonance Raman and optical absorption spectroscopies. In contrast to the monooxygenase chemistry of P450s, the dioxygenase reactions of TDO and IDO are relatively unexplored. Our results provide the first glimpse of the mechanistic insights of the dioxygenase chemistry carried out by the two enzymes. Recently, hIDO has been recognized as an important drug target for cancer and neurological disorders;[8,25,26,35−37] the differences between hIDO and hTDO revealed in this work hence offer invaluable structural information for the design of new inhibitors selective for hIDO.

Materials and Methods

Expression and Purification of hTDO. The details of protein expression and purification are described elsewhere (Batabyal et al., manuscript in preparation). Briefly, the hTDO protein, with truncated N- and C-terminal tails, plus a 6X-His tag extension at the C-terminus, were overexpressed in *E. coli* BL21 Star (DE3) cells by using the pET14b vector (Stratagene, La Jolla, CA). The recombinant protein was purified by affinity chromatography with an Ni-NTA column (Novagen). The protein was eluted with 250−300 mM imidazole (Sigma) in 50 mM phosphate buffer (pH 7.8), which was subsequently removed by dialysis. To stabilize the protein, 10 mM L-Trp was present throughout the purification procedure. The protein thus collected was stored in 50 mM phosphate buffer (pH 7.8, 10 mM L-trp) with 10% glycerol at liquid nitrogen temperature until use. To ensure that the protein was in its ferric L-Trp free state, before each experiment, it was oxidized with potassium ferricyanide, and subsequently passed through a sephadex G25 column to remove the ferricyanide, L-Trp and glycerol.

Activity Assay. For the activity measurements, the ferric hTDO was rapidly mixed with a desired amount of D-Trp or L-Trp in the presence of 100 μM sodium ascorbate in pH 7.0 phosphate buffer (100 mM) at room temperature. The final concentration of hTDO was 0.5 μM. The reaction was followed by monitoring the rate of product formation at 321 nm (ϵ = 3750 M^{-1} cm^{-1} for *N*-formyl kynurenine).[12] The K_m and k_{cat} values were determined by Michaelis−Menten curve fit of the data by using Origin 6.1 software (Microcal Software, Inc., MA). All chemical reagents were obtained from Sigma-Aldrich and were of the highest available purity.

Spectroscopic Measurements. The optical absorption spectra were taken on a spectrophotometer (UV2100U) from Shimadzu Scientific Instruments, Inc. (Columbia, MD) with a spectral slit width of 1 nm. The resonance Raman spectra were taken on the instrument described elsewhere.[38] Briefly, the 413.1 nm excitation from a Kr ion laser (Spectra Physics, Mountain View, CA) was focused to a ~30 μm spot on the spinning quartz cell rotating at ~1000 rpm. The scattered light, collected at right angle to the incident laser beam, was focused on the 100-μm wide entrance slit of a 1.25 m Spex spectrometer equipped with a 1200 grooves/mm grating (Horiba Jobin Yvon, Edison, NJ), where it was dispersed and then detected by a liquid-nitrogen cooled CCD detector (Princeton Instruments, Trenton, NJ). A holographic notch filter (Kaiser, Ann Arbor, MI) was used to remove the laser scattering. The Raman shift was calibrated by using indene (Sigma) and an acetone/ferrocyanide (Sigma) mixture as the references for the 200−1700 and 1600−2200 cm^{-1} spectral windows, respectively. The laser power was kept at ~5 mW for all measurements, with the exception of that used for the CO complexes, which was kept at ~1−2 mW to avoid photodissociation of the heme-bound CO. The acquisition time was ~20−30 min for all of the spectra obtained, with the exception of that used for the measurements of the ν_{C-O} mode, which was ~1−2 h.

The ferrous derivative was prepared by reduction of the ferric protein, pre-purged with Ar gas, with dithionite under anaerobic conditions. The CO- or NO-bound ferrous complexes were obtained by gentle purging CO or NO gas on the surface of the solution containing the ferrous form of the enzyme under anaerobic conditions. The concentration of the protein samples used for the Raman measurements was ~15−50 μM in pH 7.0 phosphate buffer (100 mM). The $^{12}C^{16}O$ and $^{14}N^{16}O$ were obtained from Tech Air (White Plains, NY), and the $^{13}C^{16}O$ and $^{15}N^{16}O$ were purchased from Icon Isotopes (Summit, NJ).

Results and Discussion

Optical Absorption Spectra of hTDO. Figure 2A shows the optical absorption spectra of the exogenous ligand-free ferric and ferrous derivatives, as well as the CO-bound ferrous derivative of hTDO. The ferric protein shows a Soret maximum at 406 nm and a visible band at 633 nm (Table 1), typical for a six-coordinate water-bound heme species. The ferrous protein shows a Soret maximum at 432 nm and a single visible band at 556 nm, consistent with a five-coordinate high-spin ferrous heme species. The CO-bound protein, on the other hand, exhibits a Soret maximum at 420 nm and α and β bands at 568 and 538 nm, respectively, indicating a six-coordinate low-spin heme.

L-Trp-binding to hTDO induces small changes to the optical absorption spectra, as shown in Figure 2B. The ferric derivative shows a 1-nm shift of the Soret maximum to 407 nm, which is associated with the disappearance of the visible band at 633 nm. The ferrous and CO-derivatives also exhibit 1-nm shift in the Soret maximum to 433 and 421 nm, respectively, and the visible bands shift to 555 and 567/537 nm, respectively.

Similar measurements were carried out for the NO-bound ferrous complex, which shows Soret and α/β bands at 416 nm and 573/542 nm, respectively, for the substrate-free enzyme. L-Trp binding to the NO-bound hTDO induces 2 nm shift of the Soret maximum to 418 nm, whereas the α/β bands stay unaltered (see Figure S2 of the Supporting Information).

As listed in Table 1, the electronic transition bands of hTDO revealed in this work are comparable to those of other heme-containing proteins with histidine as the heme proximal ligand, including hIDO. Nonetheless, the spectral perturbation introduced by L-Trp binding in hTDO appear to be much less

(34) Aitken, J. B.; Thomas, S. E.; Stocker, R.; Thomas, S. R.; Takikawa, O.; Armstrong, R. S.; Lay, P. A. *Biochemistry* **2004**, *43*, 4892−4898.
(35) Gaspari, P.; Banerjee, T.; Malachowski, W. P.; Muller, A. J.; Prendergast, G. C.; DuHadaway, J.; Bennett, S.; Donovan, A. M. *J. Med. Chem.* **2006**, *49*, 684−692.
(36) Pereira, A.; Vottero, E.; Roberge, M.; Mauk, A. G.; Andersen, R. J. *J. Nat. Prod.* **2006**, *69*, 1496−1499.
(37) Botting, N. P. *Chem. Soc. Rev.* **1995**, *24*, 401−412.
(38) Egawa, T.; Yeh, S. R. *J. Inorg. Biochem.* **2005**, *99*, 72−96.

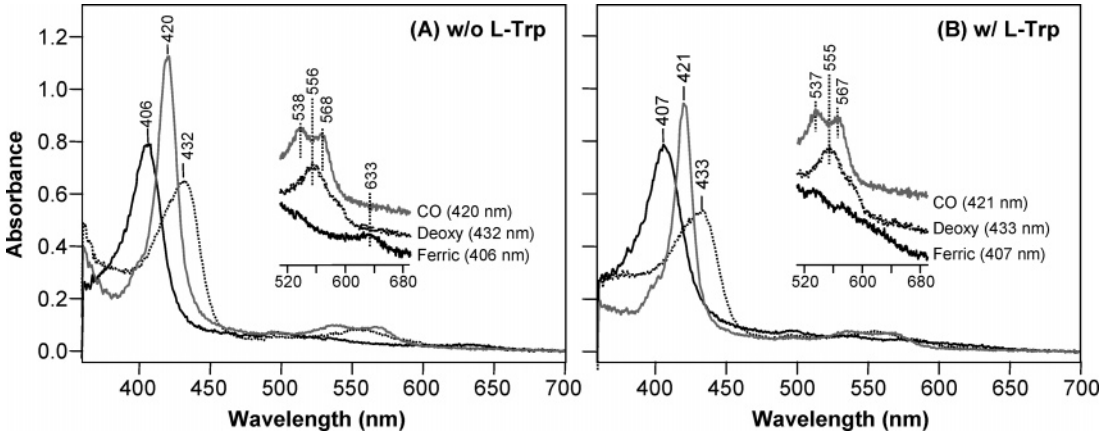

Figure 2. Optical absorption spectra of the ferric, ferrous and CO-bound hTDO in the absence (A) and presence (B) of L-Trp. The protein was in pH 7.0 phosphate buffer. The concentration of L-Trp was 5 mM. The inserts are the expanded views of the visible bands.

Table 1. Iron-Ligand Vibrational Frequencies (cm^{-1}) and Soret and Visible Absorption Maxima (nm) of hTDO and hIDO as Compared to HRP, Hb, and Mb

		υ_{Fe-His}	υ_{Fe-CO}	υ_{C-O}	A_{ferric}[a]	$A_{ferrous}$[a]	A_{CO}[a]	A_{NO}[a]	ref
TDO	substrate-free	229	496	1958	406	432	420	416	this work
					633	556	538/568	542/573	
	L-Trp	229	488	1972	407	433	421	418	this work
						555	537/567	542/573	
	D-Trp	nd	490	nd	406	432	421	nd	this work
						558	569		
	1-methyl-L-Trp	nd	488	nd	407	431	421	nd	this work
						558	538/569		
hIDO	substrate-free	236	518	1933	404	429	420	417, 542/ 570	32, *b*
					535/633	557	539/570		
	L-Trp	236	542	1901	411	425	416	415, 542/ 570	32, *b*
					540/576	556	538, 568		
HRP		244	541	1906	403	437	423	421	63, 64
					497/642	556	542/573	542/570	
HbA		215	507	1951	405	430	419	418	65, 66
					500/631	555	540/565	545/575	
Mb		220	512	1944	410	434	423	421	65
					505,635	556	542/579	543/575	

[a] The *A* values are the absorption maxima of the Soret and visible bands. [b] Samelson-Jones et al., unpublished results.

significant as compared to those observed in hIDO, indicating a weaker substrate−protein interaction in hTDO as will be discussed in more detail later.

Activity of hTDO. To quantify the activity of hTDO, we rapidly mixed the fully oxidized enzyme with a desired amount of L-Trp in the presence of 100 μM sodium ascorbate (as the reductant for hTDO) and followed the product formation as a function of time by monitoring the absorbance at 321 nm (ϵ = 3750 M^{-1} cm^{-1} for NFK).[12] Figure 3A shows a typical time course for the production of the NFK following the initiation of the reaction. In the pre-steady-state region, a small lag-phase was observed. It was followed by a linear steady-state kinetic phase, with a slope of 1×10^{-3} mM/s, as indicated by the light gray line. The linear velocity was measured as a function of L-Trp concentration and plotted in Figure 3B. The data exhibit a classical saturation behavior and can be fitted with the Michaelis−Menten equation with k_{cat} = 2.1 s^{-1} and K_m = 0.19 mM. These values are comparable to those of rat liver enzyme as listed in Table 2.

To investigate the stereospecificity of hTDO, we examined the activity of hTDO toward D-Trp. As shown in Figure 3A, the activity of hTDO toward D-Trp is significantly lower than L-Trp. The Michaelis−Menten curve fit of the D-Trp data (Figure 3B) indicate that the K_m value, 0.18 mM, is similar to that of L-Trp, whereas the k_{cat} value, 0.2 s^{-1}, is 10-fold lower than that of L-Trp (2.1 s^{-1}).

It has been shown that the purified TDO from mouse liver acted on both D-Trp and L-Trp, whereas the *Pseudomonad* and *Xanthomonas* isoforms are strictly specific for the L-isomer.[10,39] Subsequent studies demonstrated that the stereospecificity of TDO varies a great deal from species to species, among which the TDO in rat liver and human liver extracts exhibit ~7 and 25% activity, respectively, toward D-Trp as compared to L-Trp.[39] The data reported here suggest that the stereospecificity of hTDO is mainly determined by the efficiency of the dioxygen chemistry (k_{cat}), rather than the affinity of the substrate (K_m).

Despite of the fact that in the postulated reaction cycle of TDO, only the ferrous derivative is active (see right panel in Scheme 1), we found that in the absence of ascorbate, the ferric hTDO also exhibits significant activity toward L-Trp, although it is inactive toward D-Trp. The activity is not a result of residual reduced enzyme, since hTDO was pretreated with a strong oxidant, potassium ferricyanide, prior to use (see the Materials and Methods section). In addition, similar activity of the ferric derivative of TDO has been reported by Li et al. for mosquito

(39) Watanabe, Y.; Fujiwara, M.; Yoshida, R.; Hayaishi, O. Stereospecificity of hepatic L-tryptophan 2,3-dioxygenase. *Biochem. J.* **1980**, *189*, 393−405.

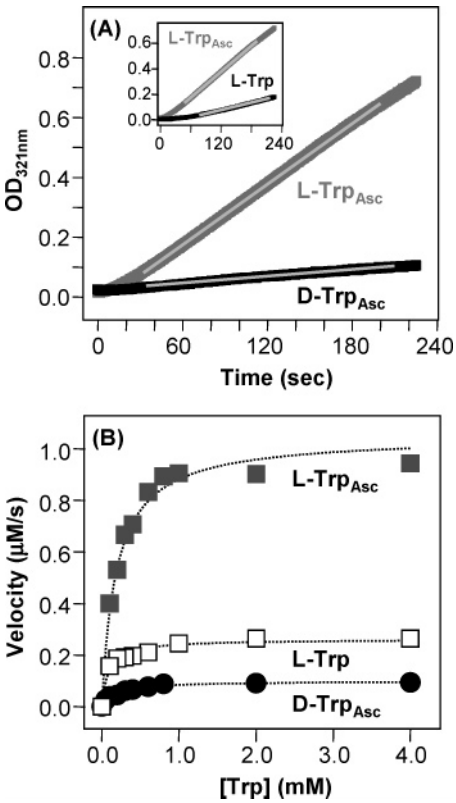

Figure 3. Formation of *N*-formyl kynurenine as a function of time during the reaction of hTDO with L-Trp (with and without ascorbate) and D-Trp (A) and the associated Michaelis-Menten plots (B). In (A), the light gray lines are the linear fits of the steady-state data. The concentration of L-Trp and D-Trp was 2 mM. The inset shows the effect of ascorbate in the product formation rate. In (B), the dotted lines show the Michaelis−Menten curve fits of the data. The concentrations of protein and ascorbate were 0.5 μM and 100 μM, respectively. The reaction was initiated by adding the protein into the reaction mixture in pH 7.0 phosphate buffer.

Table 2. Michaelis−Menten Parameters, K_m and k_{cat}, of the TDO and IDO Enzymes from the Various Species

	species	substrate	pH	K_m (mM)	k_{cat} (s^{-1})	ref
TDO	human	L-Trp	7.0	0.19	2.1	this work
		D-Trp	7.0	0.18	0.2	this work
		L-Trp[a]	7.0	0.18	0.6	this work
	Xanthomonas	L-Trp	7.5	0.114	19.5	10
		D-Trp	7.5	0.016	0	10
	Pseudomonas	L-Trp	7.0−7.5	0.7	18	18, 67
	rat	L-Trp	6	1.0	3−4	13, 18
			8	0.3		
IDO	human	L-Trp	6.5	0.021	1.7	68
		D-Trp	6.5	14	4.9	68
	rabbit (I)[b]	L-Trp	6	0.050	2	6, 69
			7	0.013		
		D-Trp	6	7.4	1.6	6, 69
			7	1.7		
			8	0.8		
	rabbit (II)[b]	L-Trp	6.6	0.045	1.7	23
		D-Trp	7.8	0.4	1.18	23

[a] Obtained in the absence of the reductant, ascorbate. [b] The data obtained from two different references as indicated.

TDO.[11] As shown in Figure 3A, without ascorbate, the kinetic trace exhibits an extended lag-phase, suggesting that the multiple turnover of the reaction under the non-reducing condition is somehow rate-limited by the reduction of the heme iron. The Michaelis−Menten curve fit of the data (Figure 3B) shows that the K_m and k_{cat} values are 0.18 mM and 0.6 s^{-1}, respectively.

It is interesting to note that, in contrast to hTDO, the ferric derivative of hIDO in the absence of reductant exhibits activity toward D-Trp, but not L-Trp (Samelson-Jones et al., unpublished results). Although the exact activation mechanisms of the ferric hTDO and hIDO by L-Trp and D-Trp, respectively, remain to be further investigated, possible source of electron responsible for the activity of the ferric proteins may be the substrate, L-Trp, itself or an amino acid of the protein located in the proximity of the heme irons.

Resonance Raman Studies. To unveil the structural properties of hTDO, we employed resonance Raman spectroscopy to examine the various derivatives of the enzyme. The general characteristics of the resonance Raman spectra of heme-proteins have been well established.[38,40−43] The high-frequency region of the spectrum is dominated by the porphyrin in-plane totally symmetric vibrational modes. Among them, the ν_2 mode in the 1550 and 1600 cm^{-1} region is sensitive to the spin-state of the heme iron, whereas the ν_3 mode in the 1475−1520 cm^{-1} region is sensitive to both the spin-state and the axial-coordination state of the iron. On the other hand, the strong ν_4 mode in the 1350 and 1400 cm^{-1} region is sensitive to the oxidation state of the heme iron as well as the π-electron density of the porphyrin macrocycle. Additional bands in the low-frequency region of the spectrum (200−1000 cm^{-1}), including iron-ligand stretching modes, bending modes associated with propionate and vinyl groups peripheral to the heme and heme out-of-plane modes, offer valuable structural information regarding the active site structures of heme-proteins, since these modes are typically sensitive to H-bonding, hydrophobic and/or steric interactions imposed on the heme group by its surrounding protein matrix.

Ferric Derivative. Figure 4 shows the resonance Raman spectrum of the substrate-free ferric hTDO. In the high-frequency region, the ν_4, ν_3, and ν_2 modes are identified at 1371, 1482, and 1560 cm^{-1}, respectively, characteristic for a six-coordinate water-bound high-spin ferric heme.[40,41,44] The bands at 1516 and 1582 cm^{-1}, which have been reported in other six-coordinate high-spin heme, are porphyrin modes instead of iron spin-state marker lines.[45] In the low-frequency region of the spectrum, the strong 677 cm^{-1} band is assigned to the ν_7 mode, whereas the 338 cm^{-1} band is identified as the ν_8 mode.[46] On the other hand, the band at 385 cm^{-1} is attributed to the bending mode of the propionate groups ($\delta_{propionate}$) and that at 422 cm^{-1} is the in-plane bending mode of the vinyl groups (δ_{vinyl}) of the heme.[46]

Addition of L-Trp to hTDO causes small shift of the ν_4 mode from 1371 to 1375 cm^{-1}, and a small increase in the six-coordinate low-spin component as indicated by the enhancement of the ν_2 mode at 1583 cm^{-1} with respect to that at 1560 cm^{-1} and the appearance of the ν_3 at 1506 cm^{-1}. The small shoulder on the low-frequency side of the ν_4 mode (as indicated by the

(40) Spiro, T. G.; Li, X. Y. In *Biological Applications of Raman Spectroscopy*; John Wiley and Sons: New York, 1988.
(41) Wang, J.; Caughey, W. S.; Rousseau, D. L. In *Methods in Nitric Oxide Research*; John Wiley & Sons: New York, 1996; pp 427−454.
(42) Kitagawa, T.; Ozaki, Y. *Struct. Bond.* **1987**, *64*, 71−114.
(43) Yu, N.-T.; Kerr, E. A. In *Biological Applications of Raman Spectroscopy: Resonance Raman Spectra of Hemes and Metalloproteins*; Spiro, T. G., Ed.; John Wiley & Sons, New York, 1988; pp 39−95.
(44) Feis, A.; Marzocchi, M. P.; Paoli, M.; Smulevich, G. *Biochemistry* **1994**, *33*, 4577−4583.
(45) Henry, E. R.; Rousseau, D. L.; Hopfield, J. J.; Noble, R. W.; Simon, S. R. *Biochemistry* **1985**, *24*, 5907−5918.
(46) Hu, S.; Smith, K. M.; Spiro, T, G. *J. Am. Chem. Soc* **1996**, *118*, 12368−12646.

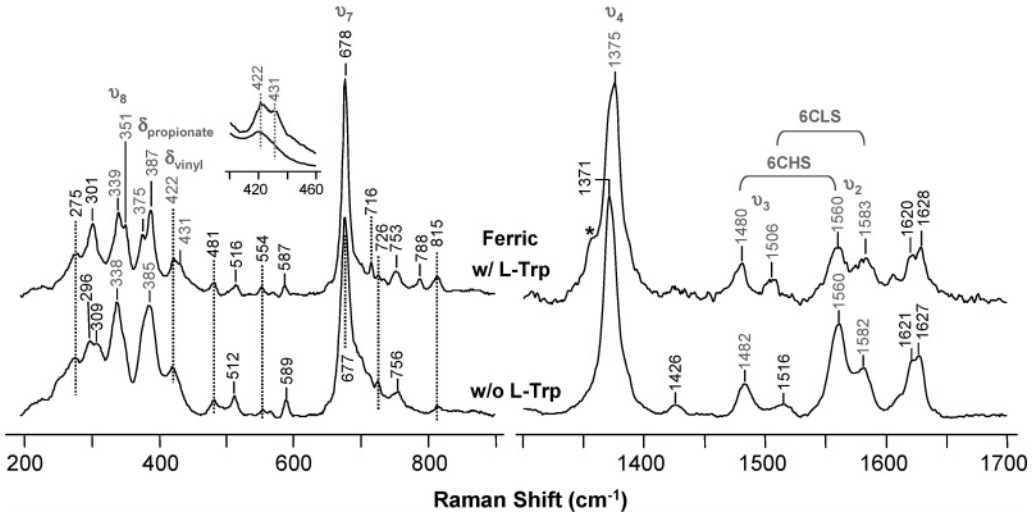

Figure 4. Resonance Raman spectra of the ferric-derivative of hTDO in the presence and absence of L-Trp. The insert is an expanded view of the δ_{vinyl} modes. The excitation wavelength was 413.1 nm and the laser power was ~5 mW. The concentration of L-Trp was 5 mM. The aster indicates the small amount of reduced protein as a result of photoreduction.

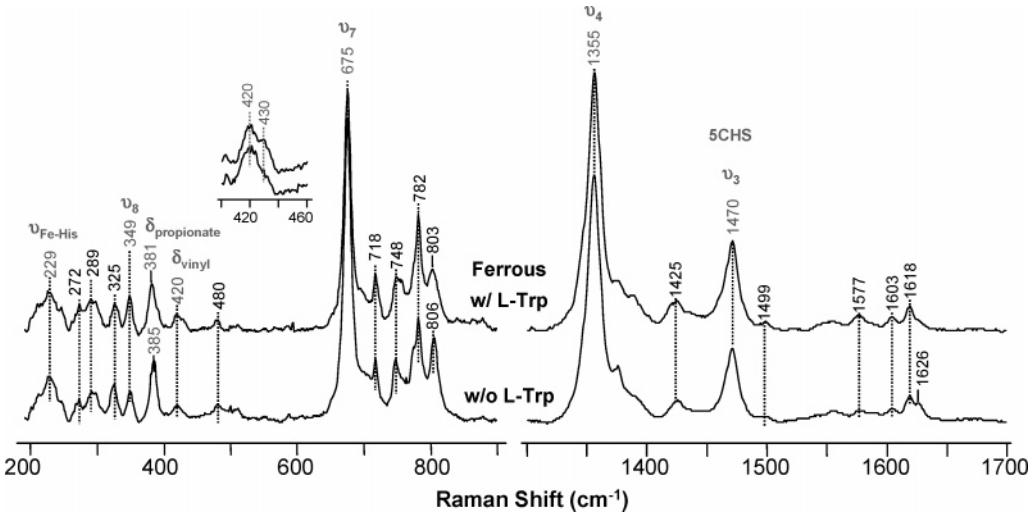

Figure 5. Resonance Raman spectra of the ferrous-derivative of hTDO in the presence and absence of L-Trp. The insert is an expanded view of the δ_{vinyl} modes. The excitation wavelength was 413.1 nm and the laser power was ~5 mW. The concentration of L-Trp was 5 mM.

aster) is due to the presence of a minute amount of reduced protein as a result of photoreduction. Although a significant amount of high-spin component is present in the Raman spectrum, the high-spin marker line at 633 nm totally disappears in the electronic absorption spectrum (Figure 2B), presumably due to its low extinction coefficient. The increase in the low-spin component in response to L-Trp binding suggests that the substrate, L-Trp, binds in the vicinity of the heme-bound water, thereby lowering its pk_a and partially converting the water (a weak field ligand) to a hydroxide (a strong field ligand). In hIDO, addition of L-Trp leads to a much more pronounced increase in the low-spin component[32] as compared to hTDO, suggesting that the L-Trp creates a relatively weaker positive polar environment for the heme-bound water in hTDO.

In addition to the spin-transition, L-Trp binding in hTDO also leads to the splitting of the δ_{vinyl} mode at 421 cm^{-1} into two bands at 422 and 431 cm^{-1}, indicating that one of the two vinyl groups of the heme changes its conformation. The $\delta_{propionate}$ mode also converts from a single band at 385 cm^{-1} to two bands at 375 and 387 cm^{-1}, consistent with the crystallographic structural data shown in Figure 1, in which one of the two propionate groups of the heme forms an H-bond with the amino group of the L-Trp. The change in the H-bonding interaction with the propionate group may reduce the electron density on the porphyrin macrocycle as suggested by the shift of the ν_4 mode from 1371 to 1375 cm^{-1}. It is noted that the 4 cm^{-1} shift is not a result of the spin-state change, because the ν_4 mode is typically not sensitive to the spin-state of the heme iron.[45]

Taken together, the resonance Raman data of the ferric derivative of hTDO indicate that L-Trp binds next to the distal ligand binding site of hTDO, and it causes partial deprotonation of the heme-bound water, which concurrently introduces conformational changes to the heme peripheral groups and the electron density on the porphyrin macrocycle.

Ferrous-Derivative. Figure 5 shows the resonance Raman spectra of the ferrous derivative of hTDO. In the high-frequency region, the ν_4 and ν_3 modes are identified at 1356 and 1471 cm^{-1}, respectively, characteristic of a 5C high-spin heme with histidine as the proximal ligand.[38] In the low-frequency region, the 229 cm^{-1} band is assigned to the proximal Fe-His stretching mode (ν_{Fe-His}). The ν_{Fe-His} frequency is significantly higher than

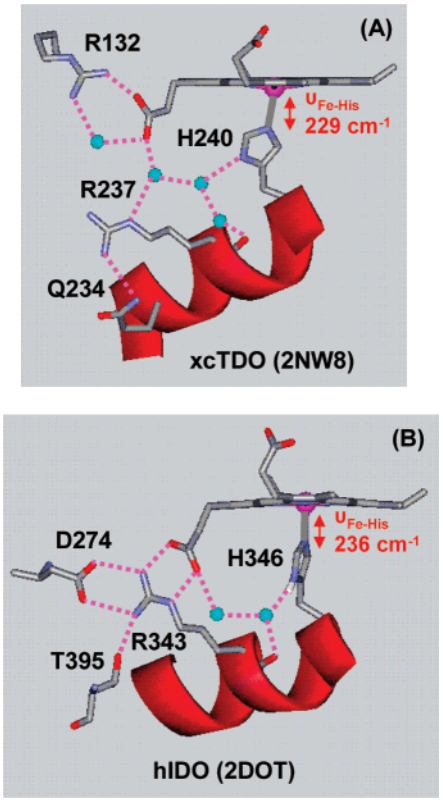

Figure 6. Proximal H-binding interactions in hTDO (A) and hIDO (B). The PDB codes of the two structures are as indicated. The magenta dotted lines represent H-bonds. The cyan spheres are water molecules. The xcTDO structure is of the L-Trp-bound enzyme with five coordinate ferrous heme and the hIDO structure is of the L-Trp-free enzyme with six-coordinated ferric heme with 4-phenylimidazole as the distal ligand. The proximal iron histidine stretching frequencies (ν_{Fe-His}) indicated were taken from hTDO in (A) and hIDO in (B).

that observed for globins (~215−220 cm^{-1}), but is lower than that of the peroxidases (~235−245 cm^{-1})[41,47,48] and hIDO (236 cm^{-1}).[32]

In hIDO, the proximal His346 donates an H-bond to a water molecule (Figure 6B), which withdraws a proton from the histidine and introduces imidazolate character to the histidine, thereby accounting for the peroxidase-like high ν_{Fe-His} frequency.[32,49] The interaction between the His346 and the water molecule is secured by an extended H-bonding network involving an additional water molecule, the Arg343, Asp274, and Thr395 residues and a propionate group of the heme. Interestingly, a similar H-bonding network, involving four water molecules, the Arg237, Arg132, and Gln234 residues and a propionate group of the heme, is also present in the structure of TDO as shown in Figure 6A. Like hIDO, the H-bonding network accounts for the relatively high ν_{Fe-His} frequency of hTDO with respect to globins. On the other hand, the lower ν_{Fe-His} frequency of hTDO with respect to hIDO indicates that the H-bonding network in hTDO is weaker than that in hIDO. It is important to note that although heme oxidation and coordination states may affect the H-bonding network, the structure of hIDO we used here is of 4-phenylimidazole-bound ferric enzyme, because it is the only crystal structure available for hIDO, whereas that of xcTDO is of L-Trp-bound ferrous enzyme.

Addition of L-Trp does not change the spin and coordination states of the ferrous heme iron, as indicated by the unaltered ν_4 and ν_3 modes at 1355 and 1470 cm^{-1}, respectively. However, it causes the enhancement of the shoulder of the δ_{vinyl} mode at 430 cm^{-1}, indicating that one of the two vinyl groups of the heme changes its conformation as observed in the ferric protein, although the ν_{Fe-His} mode at 229 cm^{-1} is not disturbed at all. Trp-binding also induces the shift of the $\delta_{propionate}$ mode from 385 to 381 cm^{-1}, indicating the changes in the conformations of propionate groups of the heme.

NO-Bound Ferrous Derivative. NO is a useful structural probe for the distal ligand binding pocket of heme-proteins. It is a strong field ligand, which is capable of binding both ferric and ferrous hemes.[38,41] The NO-bound ferric derivative of hTDO is prone to auto-reduction, especially in the presence of L-Trp, making spectroscopic measurements a nontrivial task. Here, we report the resonance Raman spectra of the NO-bound ferrous derivative of hTDO. As shown in Figure 7A, the 447 and 555 cm^{-1} bands are assigned to the Fe−NO stretching mode (ν_{Fe-NO}) and Fe−NO bending mode (δ_{Fe-N-O}), respectively, based on the $^{14}N^{16}O-^{15}N^{16}O$ isotope difference spectrum shown in Figure 7B. In the isotope difference spectrum, all of the heme modes are cancelled out, and the remaining positive and negative bands are the vibrational modes associated with $^{14}N^{16}O$ and $^{15}N^{16}O$, respectively. Although the assignment of the NO related stretching and bending modes are controversial due to the bent nature of the Fe−N−O moiety and the possible mixing of the two modes,[41,50,51] here we adopt the assignment reported by Zeng et al. for the myglobin (Mb) system.[51]

The $^{14}N^{16}O-^{15}N^{16}O$ isotope difference spectrum of the substrate-free hTDO shown in Figure 7B is almost identical to that of Mb,[52] suggesting that the Fe−N−O moiety, like that in Mb, adopts a bent conformation and the heme-bound NO accepts an H-bond from a nearby residue, possibly the His55 as illustrated in the insert in Figure 7A. As the His55 in hTDO is replaced by a serine in hIDO,[19] this H-bond is not present in hIDO, which may account for the spectral differences between the two enzymes (see the bottom traces in Figure 7, parts B and C).

L-Trp binding to the NO-bound hTDO causes the disappearance of the ν_{Fe-NO} mode at 447 cm^{-1} and the shift of the δ_{Fe-NO} mode from 555 to 571 cm^{-1} (Figure 7A), indicating that L-Trp binds in the vicinity of the heme-bound NO, thereby affecting its conformation. In contrast, L-Trp binding to the NO-bound hIDO causes the two δ_{Fe-N-O} modes to emerge into one band at 579 cm^{-1}, and the appearance of the ν_{Fe-NO} mode at 463 cm^{-1} (Figure 7C), due to the formation of an H-bond between the indole NH group of the L-Trp and the heme-bound NO.[49] This H-bond is perhaps not present in hTDO, as suggested by the Raman data of the CO-derivatives (*vide infra*), which may be responsible for the observed spectral differences between the two dioxygenases (see the top traces in Figure 7, parts B and C).

(47) Smulevich, G. In *Biomolecular Spectroscopy, Part A*; John Wiley and Sons: New York, 1993; pp 163−193.
(48) Yu, N. T.; Kerr, E. A. In *Biological Applications of Raman Spectroscopy*; John Wiley and Sons: New York, 1988; pp 39−95.
(49) Samelson-Jones, B. J.; Yeh, S. R. *Biochemistry* **2006**, *45*, 8527−38.
(50) Vogel, K. M.; Kozlowski, P. M.; Zgierski, M. Z.; Spiro, T. G. *J. Am. Chem. Soc.* **1999**, *121*, 9915−9921.
(51) Zeng, W.; Silvernail, N. J.; Wharton, D. C.; Georgiev, G. Y.; Leu, B. M.; Scheidt, W. R.; Zhao, J.; Sturhahn, W.; Alp, E. E.; Sage, J. T. *J. Am. Chem. Soc.* **2005**, *127*, 11200−11201.
(52) Tomita, T.; Hirota, S.; Takashi, O.; Olson, J. S.; Kitigawa, T. *J. Phys. Chem. B* **1999**, *103*, 7044−7054.

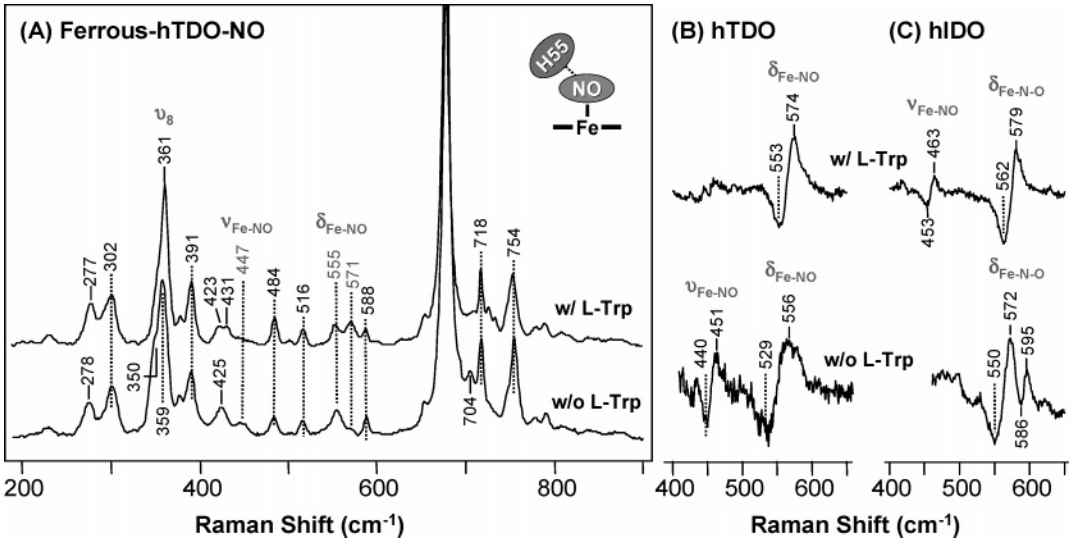

Figure 7. Resonance Raman spectra of the NO-bound ferrous derivative of hTDO in the presence and absence of L-Trp (A) and the $^{14}NO-^{15}NO$ isotope difference spectra of hTDO (B) and hIDO (C). In the isotope difference spectrum, all of the heme modes are cancelled out; the remaining peaks are associated the ν_{Fe-NO} and δ_{Fe-N-O} modes as indicated. The excitation wavelength was 413.1 nm and the laser power was ~5 mW. The concentration of L-Trp was 5 mM. The insert in (A) illustrates the H-bonding interaction between the heme-bound NO and the distal His55 in the substrate-free hTDO. The data in (C) are adopted from literature[49] as a comparison.

CO-Bound Ferrous Derivative. CO, like NO, is a strong-field ferrous heme ligand and is an important structural probe for ligand binding pocket of heme-proteins. In contrast to the bent geometry of the Fe−N−O moiety, the Fe−C−O moiety typically adopts a linear structure; therefore, it provides structural information complementary to that offered by the NO-complex. Figure 8A shows the resonance Raman spectra of the CO-complex of hTDO. In the substrate-free enzyme, the broad band centered at ~496 cm^{-1} is assigned to the Fe−CO stretching mode (ν_{Fe-CO}), as manifested in the $^{12}C^{16}O-^{13}C^{16}O$ isotope difference spectrum shown in Figure 8B. The small band at 579 cm^{-1}, which shifts to ~553 cm^{-1} upon the isotope substitution, is assigned to the Fe−CO bending mode (δ_{Fe-C-O}), on the basis its absolute frequency as well as the degree of the isotopic shift. An additional isotope sensitive mode at 1958 cm^{-1}, which shifts to 1913 cm^{-1} upon the substitution of $^{12}C^{16}O$ with $^{13}C^{16}O$, is assigned as the C−O stretching mode (ν_{C-O}) as shown in Figure 8C.

Addition of L-Trp leads to the disappearance of the δ_{Fe-C-O} mode and the sharpening as well as the shift of the ν_{Fe-CO}/ν_{C-O} modes from 496/1958 cm^{-1} to 488/1972 cm^{-1} (Figure 8). It is noted that the band at ~570 cm^{-1} is a porphyrin mode, instead of the δ_{Fe-C-O} mode, as it does not show any CO isotope sensitivity.

When CO binds to heme-proteins, it donates electrons to the heme iron to form the σ bond, which greatly increases the electron density on the heme iron. To stabilize the Fe−C−O moiety, the excess electron density on the heme iron is donated from its d_π orbital back to the π^* orbital of the CO (the so-called π back-bonding effect).[38,41,43,53] As a result, the Fe−C−O moiety can be presented by the following two structures.

$$Fe^{\delta-}-C\equiv O^{\delta+}\ (I) \leftrightarrow Fe=C=O\ (II) \qquad (1)$$

The degree of π back-bonding is modulated by the protein matrix surrounding the CO moiety. As a general rule, a positive polar environment destabilizes form (I) and facilitates the π back-bonding interaction. Consequently, the bond-order of the Fe−CO is increased, which is concurrent with a decrease in the bond-order of the C−O. On this basis, the ν_{Fe-CO} and ν_{C-O} frequencies are typically inversely correlated, as shown in Figure 9A for heme-proteins with histidine as the proximal ligand. In heme-proteins with cysteine as the proximal ligand, the inverse correlation line is offset down from the histidine line as a result of the modulation in the electron density distribution on the Fe−C−O moiety.[38] Likewise, five-coordinate CO adducts of ferrous hemes fall on a distinct inverse correlation line that sits above the histidine line. Due to its sensitivity to the identity of the proximal heme ligand, as well as the distal environment, CO has been widely recognized as a useful structural probe for heme-proteins.

The data point of hTDO, with ν_{Fe-CO}/ν_{C-O} at 496/1958 cm^{-1}, lies on the inverse correlation line associated with heme-proteins with histidine as the proximal ligand, confirming that the proximal ligand of hTDO is indeed a histidine. It is located in the lower right corner of the correlation line (Figure 9A), indicating that the ligand binding pocket has a relatively low electrostatic potential.[53,54] The binding of L-Trp to hTDO shifts the data point to an even lower position, indicating that L-Trp binds in the vicinity of the heme-bound CO, thereby further lowering the electrostatic potential of the environment surrounding it.

In contrast to hTDO, the data points associated with peroxidases, such as HRP (horse radish peroxidase), typically lie in the upper left corner of the correlation line due to the presence of the H-bonds between the heme-bound CO and the two distal polar residues, His42 and Arg38.[55] The positive polar distal environment has been shown to play a critical role in facilitating the O−O bond cleavage reaction essential for the peroxidase activity.[56,57] The data presented here hence clearly demonstrates

(53) Spiro, T. G.; Wasbotten, I. H. *J. Inorg. Biochem.* **2005**, *99*, 34−44.
(54) Li, T.; Quillin, M. L.; Phillips, G. N., Jr.; Olson, J. S. *Biochemistry* **1994**, *33*, 1433−1446.
(55) Feis, A.; Rodriguez-Lopez, J. N.; Thorneley, R. N.; Smulevich, G. *Biochemistry* **1998**, *37*, 13575−13581.
(56) Smullevich, G. F. A.; Howes, B. D. *Acc. Chem. Res.* **2005**, *38*, 433−440.
(57) Poulos, T. L.; Kraut, J. *J. Biol. Chem.* **1980**, *255*, 8199−8205.

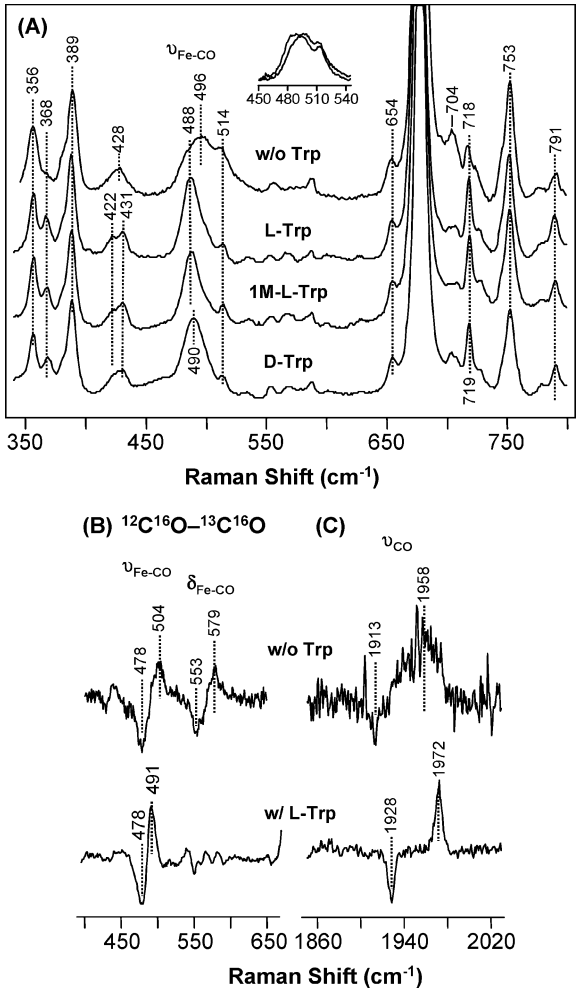

Figure 8. Resonance Raman spectra of the CO-bound hTDO in the presence and absence of the various substrates (A), and the $^{12}CO-^{13}CO$ isotope difference spectra of hTDO in the presence and absence of L-Trp (B−C). The insert in (A) shows the comparison of the ν_{Fe-CO} modes of the ^{12}CO-bound (black trace) and ^{13}CO-bound (gray trace) hTDO in the absence of L-Trp. In the isotope difference spectrum, all of the heme modes are cancelled out; the remaining peaks are associated the ν_{Fe-CO}, δ_{Fe-C-O} and ν_{C-O} modes as indicated. The concentrations of L-Trp, 1-methyl L-Trp (1M-L-Trp) and D-Trp were 5, 5, and 8 mM, respectively. The excitation wavelength was 413.1 nm and the laser power was ~1−2 mW.

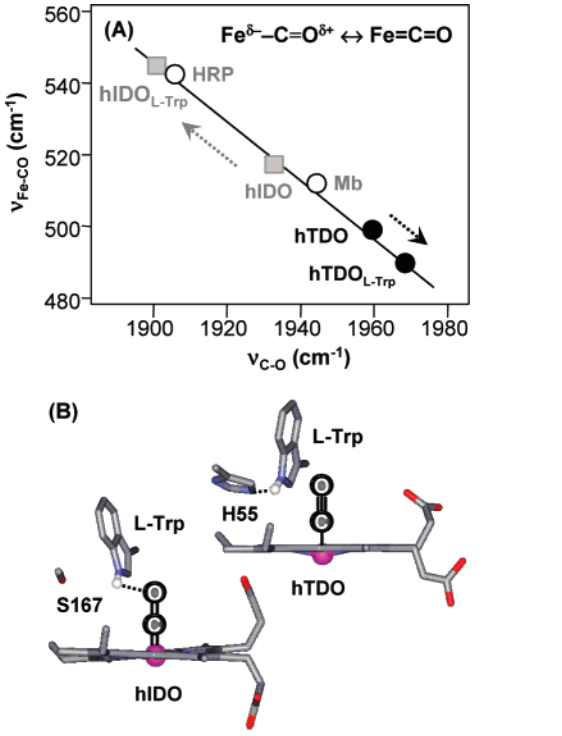

Figure 9. ν_{Fe-CO} versus ν_{C-O} inverse correlation curve (A) and pictorial illustrations of the substrate-ligand-protein interactions in hTDO and hIDO (B). The dotted arrows in (A) indicate the direction of the changes induced by L-Trp binding in hTDO and hIDO. The HRP and Mb data taken from literature (see Table 1) are presented as references. The dotted lines in (B) represent the H-bonds. In hTDO, the indole NH group of L-Trp donates an H-bond to the His55 (numbering based on the xcTDO sequence). On the basis of structure-based sequence alignment, the His55 in hTDO is replaced by Ser167 in hIDO. In hIDO, the indole NH group of L-Trp donates an H-bond to the heme-bound CO as indicated.

that it carries out the dioxygen chemistry with a mechanism distinct from peroxidases.

The data point associated with hIDO, in contrast, is located in the middle of the correlation line, indicating a distal environment with medium positive electrostatic potential.[32] The binding of L-Trp shifts the data point along the correlation line to a higher position, indicating a more positive polar environment for the CO ligand.[32] This effect is opposite to that observed in hTDO, in which the data point shifts toward the opposite direction upon L-Trp binding, as indicated by the arrows in Figure 9A. The data suggest that in the L-Trp-bound hIDO, the NH group of the indole ring of the substrate forms an H-bond with the heme-bound CO,[32] as illustrated in Figure 9B, whereas in hTDO, the aromatic portion of the indole ring is in close proximity to the heme-bound CO, possibly due to the constraint put forth by the H-bonding interaction between the indole NH group and the His55 as suggested by the crystallographic data shown in Figure 1.

In hTDO, the ν_{Fe-CO} and ν_{C-O} modes become much sharper in response to L-Trp binding (Figure 8), indicating that the hydrophobic interaction between the indole ring and the heme-bound CO dramatically reduces the conformational freedom of the heme ligand. The restriction in the mobility of the heme-bound ligand suggests that, in the active ternary complex, the alignment of the O−O bond of the heme-bound dioxygen with the C_2-C_3 double bond of the L-Trp is important for the dioxygenase reaction of hTDO as illustrated in Figure 10A (*vide infra*).

Protein−Substrate Interaction. To further investigate the protein−substrate interaction, we examined the CO-complexes of hTDO in the presence of D-Trp or 1-methyl- L-Trp. Intriguingly, the addition of the methyl group on the indole nitrogen atom of L-Trp does not affect the ν_{Fe-CO} (Figure 8A), confirming that, in the L-Trp-bound complex, the indole NH group does not directly interact with the heme-bound CO. The data also indicate that the H-bonding interaction between the indole NH group of the L-Trp and His55 is not the dominant structural factor that determines the positioning of the aromatic indole ring, although it is critical for the fine-tuning of the relative position of the heme-bound dioxygen and the C_2-C_3 double bond of the L-Trp as discussed above. This conclusion is in line with the observation that L-Trp in xcTDO is held in position by the extended H-bonding network, as well as several hydrophobic contacts as highlighted in Figure 1 and Figure S1 in the Supporting Information. Similarly, possibly due to the same reason, the replacement of the L-Trp with D-Trp causes

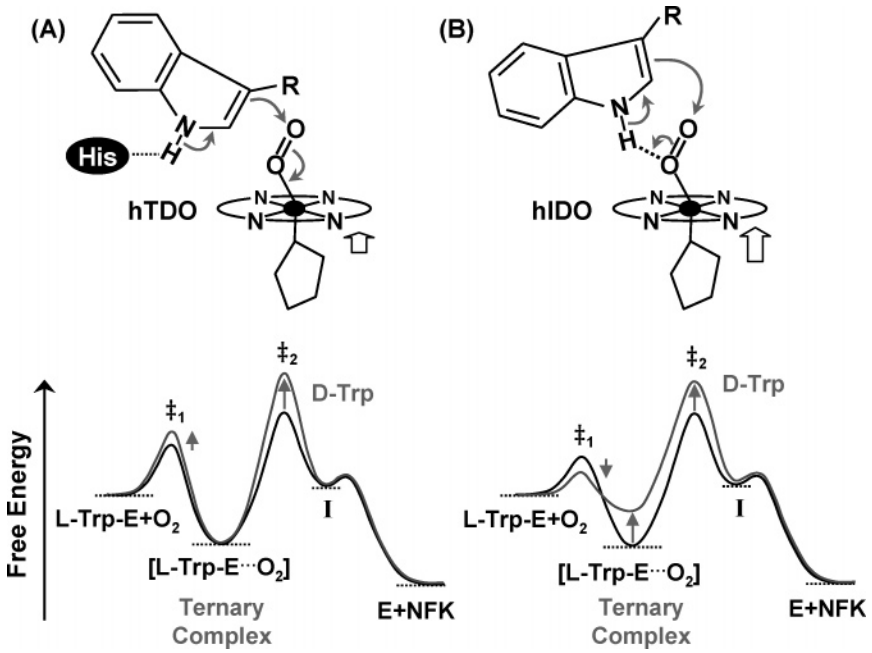

Figure 10. Postulated free energy curves associated the dioxygenase reactions of hTDO (A) and hIDO (B) with L-Trp versus D-Trp. The reaction includes the binding reaction of O_2 to Trp-bound enzyme (E) to form the active ternary complex and its subsequent conversion to the product, *N*-formyl-kynurenine (NFK), via the postulated heme iron-bound 3 indolenyl-peroxy intermediate (I). The black and gray curves are associated the reactions with L-Trp and D-Trp, respectively. The top panel shows the pictorial illustration of the postulated mechanism for the initial deprotonation reaction of L-Trp. The His in (A) represents the distal His55 (numbering based on the xcTDO sequence). The arrows indicate the electron movement required for the formation of the heme iron-bound 3 indolenyl-peroxy intermediate. The two hollow arrows on the proximal sides of the heme indicate the electronic push provided by the proximal histidine in hTDO and hIDO, respectively.

only a slight shift of the ν_{Fe-CO} from 488 to 490 cm^{-1}. It is important to note that although only a small change in the ν_{Fe-CO} frequency was observed, the k_{cat} value obtained during the multiple turnover of hTDO is 10-fold lower for D-Trp than L-Trp (Table 2), implying that the heme-bound dioxygen is not aligned with the C_2-C_3 double bond of D-Trp in an optimum orientation for the dioxygen chemistry to take place.

The substrate−protein interaction in hTDO is distinctive from hIDO. In the L-Trp-bound CO-complex of hIDO, the replacement of L-Trp with D-Trp causes the shift of the ν_{Fe-CO} frequency from 541 to 524 cm^{-1}, whereas the replacement with 1-methyl- L-Trp causes the broadening of the ν_{Fe-CO} mode (Samelson-Jones et al., manuscript in preparation). Along the same lines, hIDO has been shown to bind superoxide in its ferric state to generate the active ternary complex,[31] similar to that observed in catalase and horseradish peroxidase;[58] in contrast, hTDO, like globins, exhibits very low reactivity toward superoxide.[18] Furthermore, L-Trp-binding in hIDO retards CO binding,[30] whereas in hTDO, it facilitates CO binding.[16] Taken together, the data suggest that hIDO and hTDO carry out the dioxygenase reaction via distinct mechanisms.

Mechanistic Implications. On the basis of the ionic mechanism proposed by Hamilton,[6,59] the first step of the dioxygenase reaction of TDO and IDO involves the deprotonation of the indole NH group of Trp by an active base, as illustrated in Figure 10A (*vide infra*). The electron movement associated with the deprotonation reaction, as indicated by the gray arrows, facilitates the electrophilic addition of the heme-bound O_2 to the C_2-C_3 double bond of Trp, thereby leading to the formation of the heme iron-bound 3-indolenylperoxy intermediate, which is subsequently converted to the product, NFK, via either the dioxetane intermediate or Crieege type rearrangement, as illustrated in Figure S3 of the Supporting Information.[6,59,60]

Resonance Raman studies[32] suggest that in hIDO, the heme-bound dioxygen acts as a base for the deprotonation of the substrate L-Trp, as illustrated in Figure 10B (top). This proposal is supported by the recent crystallographic and biochemical studies reported by Sugimoto et al.[29] In contrast, our data imply that, in hTDO, L-Trp is orientated in a manner such that its C_2-C_3 double bond, rather than the indole NH group, faces the heme-bound ligand, and it is the distal His55 that deprotonates the L-Trp (Figure 10A, top). The importance of the His55 in modulating the dioxygen chemistry is supported by the observation that the dioxygenase activity of rat liver TDO decreases significantly when this conserved His residue is mutated.[61] Similarly, Forouhar et al. reported that the k_{cat} value of xcTDO decreases by a factor of 10-fold when the His55 is mutated to Ala.[10] Nonetheless, contrary to our proposal, the authors concluded that His55 in xcTDO is not essential for the L-Trp catalysis based on two arguments: (1) the observed 10-fold decrease in k_{cat} is "not" significant, and (2) the k_{cat} is insensitive to pH in the range of pH 6−8. We believe that this conclusion may not be valid, as the pH window examined may not be wide enough to cover the true pK_a of the His55, as the pK_a of His in free solution is 6.0 and the pK_a of an amino acid residue may vary a great deal in a protein matrix (especially considering the fact that the His55 forms a H-bond with the L-Trp); in addition, the 10-fold decrease in the k_{cat} is indeed significant, as it is of a similar order of magnitude as the change

(58) Shimizu, N.; Kobayashi, K.; Hayashi, K. *J. Biol. Chem.* **1984**, *259*, 4414−4418.
(59) Hamilton, G. A. *Adv. Enzymol. Relat. Areas Mol. Biol.* **1969**, *32*, 55−96.
(60) Leeds, J. M.; Brown, P. J.; McGeehan, G. M.; Brown, F. K.; Wiseman, J. S. *J. Biol. Chem.* **1993**, *268*, 17781−17786.
(61) Dick, R. M. B.; Reid, M. J.; Correia, M. A. *Arch. Biochem. Biophys.* **2001**, *392*, 71−78.

we observed when L-Trp is replaced by D-Trp as the substrate for hTDO (Table 2).

The ν_{Fe-His} frequency of hTDO reported here (229 cm^{-1}) is higher than that of globins but lower than that of peroxidases (Table 1). The high ν_{Fe-His} frequency of peroxidases has been attributed to the presence of a strong H-bond between the proximal histidine and a nearby negatively charged amino acid side-chain, which withdraws the N_ϵ proton away from the histidine, giving it the imidazolate character.[56,62] On the basis of the well-known "push−pull" model,[57] the proximal imidazolate heme ligand offers electronic push, along with the electronic pull provided by the polar distal environment, to facilitate the O−O bond cleavage required for the peroxidase reactions.[56,62] Like the peroxidases, the imidazolate character of hTDO can be attributed to the presence of the extended H-bonding network linking to the proximal histidine (Figure 6A). Nonetheless, the H-bonding interaction in hTDO is significantly weakened, presumably to avoid the premature O−O bond cleavage during the dioxygen chemistry.

The electronic push from the proximal ligand in hTDO may be important for the electron movements associated with the rearrangement reaction of the 3-indolenylperoxy intermediate to NFK via either the dioxetane or Crieege rearrangement mechanism, as may be seen in Figure S3 of the Supporting Information. However, it is plausibly disadvantageous for the electron rearrangement associated with the electrophilic addition reaction of the heme-bound O_2 to L-Trp (Figure 10A, top). The latter argument is supported by the observation that attaching electron withdrawing group on the porphyrin ring of the heme prosthetic group increases the k_{cat} of the dioxygenase reaction of TDO.[18] As such, the degree of electronic push from the proximal histidine in hTDO is probably optimized to balance the two conflicting effects.

The ν_{Fe-His} frequency of hIDO, on the other hand, is 7 cm^{-1} higher than hTDO. This may be attributed to the fact that the strong electronic push from the proximal histidine is advantageous, rather than disadvantageous, for the electrophilic addition of the heme-bound O_2 to L-Trp in hIDO as illustrated in Figure 10B (top), due to the presence of the H-bond between the indole NH group of L-Trp and the proximal oxygen atom of the heme-bound dioxygen.

As listed in Table 2, the k_{cat} value of hTDO for L-Trp is similar to that of hIDO, but the K_m of hTDO is ∼10-fold higher than that of hIDO, indicating that the affinity of hTDO for L-Trp is weaker than that of hIDO, but once the active ternary complexes are formed the two enzymes can catalyze the dioxygenase reaction with similar efficiency. On the other hand, the K_m values of hTDO for L-Trp and D-Trp are similar, whereas the k_{cat} is 10-fold higher for L-Trp than for D-Trp. In contrast, the K_m of hIDO for L-Trp is ∼700-fold lower than that of D-Trp, whereas the k_{cat} values are comparable for these two stereoisomers. These data indicate that the stereospecificity of hTDO is determined by the efficiency of the dioxygen chemistry rather than by the affinity of the substrate, whereas that of hIDO is controlled by the substrate binding affinity, instead of the dioxygen chemistry, as illustrated by the free energy curves shown in Figure 10.

In Figure 10, the dioxygenase reactions of hTDO and hIDO are described as a two-step process: the binding of dioxygen to form the active ternary complex, followed by the conversion of the L-Trp to the product, NFK, via the 3-indolenylperoxy intermediate (denoted as "I"). The activation energy barriers for the two processes are defined as $\ddagger_1$ and $\ddagger_2$, respectively. Laser flash photolysis studies of hIDO (Samelson-Jones et al., manuscript in preparation) showed that the bimolecular binding rate of CO in the L-Trp-bound enzyme is slower than the D-Trp-bound derivative (both of which are slower than the substrate-free enzyme), indicating that the $\ddagger_1$ state is stabilized upon substitution of L-Trp with D-Trp. However, the active ternary complex is destabilized, as suggested by the higher K_m value, and, concurrently, the $\ddagger_2$ state is destabilized to a similar extent (such that its relative energy to the ternary complex is only slightly perturbed), as hinted at by the comparable k_{cat} values for the two stereoisomers (Figure 10B).

In contrast to hIDO, laser flash photolysis studies of hTDO showed that the bimolecular binding rate of CO is accelerated by L-Trp binding,[16] suggesting that the $\ddagger_1$ state may be destabilized upon the substitution of L-Trp with D-Trp as illustrated in Figure 10A; at the same time, the active ternary complex is unperturbed, as suggested by the unaltered K_m value, whereas the $\ddagger_2$ state is destabilized as indicated by the lower k_{cat} value.

The distinct stereospecificity of hTDO with respect to hIDO remains to be further investigated. Nonetheless, the structural differences revealed in this work underscore the importance of the H-bonding interaction between the His55 and Trp in hTDO, which is absent in hIDO. The stabilization of the $\ddagger_1$ state and destabilization of the ternary complex in the D-Trp bound hIDO, with respect to its L-Trp-bound derivative, may be partially attributed to the absence of this H-bond.

It is worthwhile to note that the TDO enzymes of bacteria origin in general show 10-fold higher k_{cat} than those of mammalian origin (Table 2). Furthermore, recent work reported by Forouhar et al. show that, in contrast to hTDO, xcTDO exhibits a 7-fold lower affinity toward D-Trp compared to L-Trp and no catalytic activity toward D-Trp,[10] manifesting the intrinsic differences between these two classes of TDOs.

Conclusions

The data reported here show that the proximal iron-histidine bond strength of hTDO is stronger than that found in globins, but weaker than that found in hIDO. L-Trp binds to the distal heme pocket in hTDO with its C_2-C_3 double bond facing the distal heme iron-bound diatomic ligand, in contrast to hIDO, in which the indole NH group forms an H-bond with the heme ligand. The structural differences between the hTDO and hIDO revealed in this work suggest that the two dioxygenases carry out the oxidative cleavage of Trp via distinct mechanisms. In hTDO, the initial deprotonation reaction of Trp, leading to the formation of the postulated 3-indolenylperoxy intermediate, is performed by the conserved distal His55; in contrast to hIDO,

(62) Dawson, J. H. *Science* **1988**, *240*, 433−439.
(63) Keilin, D.; Hartree, E. F. *Biochem. J.* **1951**, *49*, 88−104.
(64) Yonetani, T.; Yamamoto, H.; Erman, J. E.; Leigh, J. S., Jr.; Reed, G. H. *J. Biol. Chem.* **1972**, *247*, 2447−55.
(65) Antonini, E.; Brunori, M. In *Hemoglobin and Myoglobin in Their Reactions with Ligands*; North Holland Publishing Company: Netherlands, 1971; pp 19, 44.
(66) Di Iorio, E. *Methods Enzymol.* **1981**, *76*, 57−72.
(67) Colman, P. D.; Blanchet, S. P.; Chow, E.; Feigelson, P. *J. Biol. Chem.* **1975**, *250*, 6208−6213.
(68) Takikawa, O.; Kuroiwa, T.; Yamazaki, F.; Kido, R. *J. Biol. Chem.* **1988**, *263*, 2041−2048.
(69) Sono, M. *Biochemistry* **1989**, *28*, 5400−5407.

in which the heme-bound dioxygen acts as the base to deprotonate the Trp. In hTDO, the K_m for D-Trp and L-Trp are similar, but the k_{cat} of the D-Trp is 10-fold lower than the L-Trp; in contrast, in hIDO, the K_m for D-Trp is significantly higher than that for L-Trp, whereas the k_{cat} for the two stereoisomers are comparable. The data suggest that the stereospecificity of hTDO is determined by the dioxygen chemistry, whereas that in hIDO is controlled by the binding affinity of the substrate. In summary, our data provide the first glimpse of the molecular mechanisms underlying the two heme-containing dioxygenases in humans.

Acknowledgment. This work is supported by NIH Grant No. HL65465 to S.-R.Y. We thank Dr. Denis L. Rousseau, Mr. Ben J. Samelson-Jones, Drs. Tsuyoshi Egawa, Jack Peisach, and Phil Aisen for many valuable discussions.

Supporting Information Available: Optical absorption spectra of the NO-bound ferrous hTDO in the absence and presence of 5 mM L-Trp. This material is available free of charge via the Internet at http://pubs.acs.org.

JA076186K